

Quantum Algorithm for Estimating Ollivier-Ricci Curvature

Nhat A. Nghiêm,^{1, 2, *} Linh Nguyễn,^{3, †} Tuan K. Đô,^{4, ‡} Tzu-Chieh Wei,^{1, 2, §} and Trung V. Phan^{5, ¶}

¹*Department of Physics and Astronomy, State University of New York at Stony Brook, Stony Brook, NY 11794-3800, USA*

²*C. N. Yang Institute for Theoretical Physics, State University of New York at Stony Brook, Stony Brook, NY 11794-3840, USA*

³*Department of Mathematics, Florida A&M University, Tallahassee, FL 32301, USA*

⁴*Department of Mathematics, University of California, Santa Barbara, CA 93106, USA*

⁵*Department of Natural Sciences, Scripps and Pitzer Colleges, Claremont Colleges Consortium, Claremont, CA 91711, USA*

We introduce a quantum algorithm for computing the Ollivier–Ricci curvature, a discrete analogue of the Ricci curvature defined via optimal transport on graphs and general metric spaces. This curvature has seen applications ranging from signaling fragility in financial networks to serving as basic quantities in combinatorial quantum gravity. For inputs given as a point cloud with pairwise distances, we show that our algorithm can achieve an exponential speed-up over the best-known classical methods for two particular classes of problem. Our work is another step toward quantum algorithms for geometrical problems that are capable of delivering practical value while also informing fundamental theory.

I. INTRODUCTION

The *manifold hypothesis* conjectures, with substantial empirical support, that any high-dimensional dataset can be represented by a much lower-dimensional manifold [1–3]. By stripping away redundant coordinates – often artifacts of noise or constraints [4] – one can recover the true local degrees of freedom, i.e., the intrinsic dimensionality [5]. By constructing local geometry – typically via a nearest-neighbor graph [6] and pairwise distances – we can infer the global topology of the underlying manifold and extract local geometric information such as curvature [7], whose bottlenecks or singularities flag anomalies [8]. This approach for big data analysis has many practical applications, and perhaps best known through quantitative finance, where the curvature on asset-correlation graphs are found to be a good indicator for market fragility [9, 10] and potential crash magnitude [11, 12]. Among discrete estimators of curvatures, the *Ollivier–Ricci curvature* (ORC) [13–15] has often emerged to be the most useful: it is defined via optimal transport between neighboring probability measures on the graph [16], associating curvature directly with how information moves across the network. For the same reason, ORC fits naturally with combinatorial quantum gravity [17–20], where distances and Markovian dynamics create emergent geometry. As ORC gains traction, developing efficient methods to compute it becomes essential, including novel approaches that go beyond classical algorithms.

Quantum computation has seen significant progress since its early proposals [21, 22]. By leveraging the intrinsic nature of quantum physics, including entanglement and superposition, a quantum computer can store and process information indistinguishably from a classical one. As such, it holds great promise for solving problems beyond the classical limit. Early attempts [23–26] have, to some extent, revealed such promise by showing that quantum computers can compute the property of black-box functions, search the database, and factorize integers, which can be done with considerably fewer resources than the best-known classical algorithms [27, 28]. Over time, the notion of quantum computing has reached almost every corner of scientific computing. Notable examples include solving linear systems [29–31], Hamiltonian simulation [32–40], solving differential equations [34, 41–44], machine learning & artificial intelligence [45–51], etc.

Recently, quantum algorithmic techniques have been applied in the context of topological data analysis (TDA), igniting a series of efforts [52–59]. In a parallel effort, the work [60] explores the potential of quantum computing for geometrical data analysis (GDA). While built on different mathematical grounds, TDA and GDA offer powerful frameworks for analyzing large-scale data, capable of revealing intrinsic properties of data in realistic scenarios where noise and sampling error often intervene. As outlined in the aforementioned works, quantum computers can offer an efficient solution to many problems in the TDA and GDA context, thus suggesting a broader potential for application, going beyond what was shown in the context of scientific computing, simulation, machine learning, etc.

In this work, following these developments – particularly, the attempt in [60] – we extend the reach of quantum computing to a closely relevant problem in the context of GDA. Specifically, we consider the problem of estimating ORC, given the input as a point cloud with pairwise connectivities and pairwise distances. This input

* nhatanh.nghiemvu@stonybrook.edu

† linh.nguyen@famu.edu

‡ ktdu@ucsb.edu

§ tzu-chieh.wei@stonybrook.edu

¶ tphan@natsci.claremont.edu

model is the same as [60]; however, whereas [60] estimates local scalar curvature via a diffusion-based approach, in this work, we adopt an optimal-transport-based estimator.

Our work is organized as follows. In Section II, we provide a formal description of the key objective and related assumptions. In the same section, we describe the classical solution to the key objective and state our main result, followed up by a comparison to show the advantage of our quantum method. Section III contains our main proposal for the quantum algorithm for estimating the ORC, which splits into two subsections III A and III B to handle two cases, corresponding to two different types of input conditions. Finally, conclusion is given in Section IV.

II. CLASSICAL ALGORITHM FOR CALCULATING THE OLLIVIER-RICCI CURVATURE

Consider a graph $G = (V, E)$, where V is the set of vertices and E is the set of edges. Each edge is represented by the pair of vertices it connects, $(a, b) \in E$ with $a, b \in V$, and is assigned a distance $d(a, b)$. The edges are undirected, so that $(a, b) \equiv (b, a)$. The *neighbors* of a vertex $a \in V$ are defined as the set of all vertices connected to a by an edge, i.e. $\mathcal{N}_a = \{b \in V | (a, b) \in E\}$. For any pair of vertices $a', b' \in V$, the *graph, or geodesic distance* between them, denoted $d_G(a', b')$, is defined as the length of the shortest path in G connecting a' and b' . Explicitly,

$$d_G(a', b') = \min_{\substack{(v_1, v_2), (v_2, v_3), \dots \\ (v_{k-2}, v_{k-1}), (v_{k-1}, v_k) \in E \\ v_1 = a', v_k = b'}} \sum_{i=1}^k d(v_i, v_{i+1}), \quad (\text{II.1})$$

where the minimum is taken over all possible paths in the graph G with endpoints a' and b' .

An ORC value is associated with each edge $(x, y) \in E$, denoted by $\gamma(x, y)$, and can be calculated with the Earth Mover (1-Wasserstein) distance $W_1(x, y)$ as follows [61]:

$$\gamma(x, y) = 1 - \frac{W_1(x, y)}{d_G(x, y)}. \quad (\text{II.2})$$

To calculate $W_1(x, y)$, we need to focus on the local configuration near the edge (x, y) , as illustrated in Fig. 1. Assume that the set of x -neighbors *excluding* y has p points and the set of y -neighbors *excluding* x has q points, i.e. $\mathcal{N}_x \setminus \{y\} = \{x_1, x_2, \dots, x_p\}$ and $\mathcal{N}_y \setminus \{x\} = \{y_1, y_2, \dots, y_q\}$. Then the value of $W_1(x, y)$ is the minimum cost of reconfiguring mass in vertices in $\mathcal{N}_x \setminus \{y\}$, which we further assume to sum up to 1 and be uniformly distributed, to another uniform distribution of mass in vertices in $\mathcal{N}_y \setminus \{x\}$. Concretely, denote by γ_{ij} (where $i = 1, 2, \dots, p$ and $j = 1, 2, \dots, q$) the *transport variable* that represents the amount of mass transferred from x_i

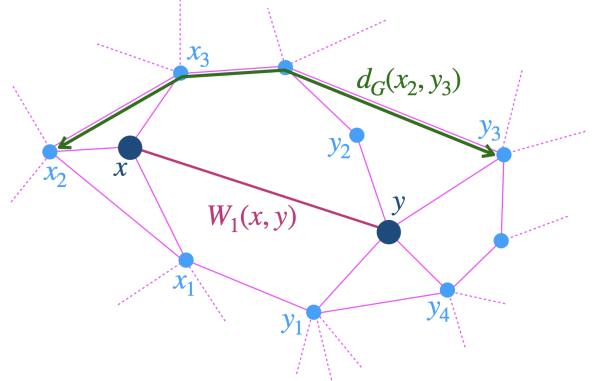


FIG. 1. Illustration of the setup used to compute the Earth Mover distance associated with an edge in a graph. The graph's vertices are in blue, and its edges are in magenta. Here we consider the edge (x, y) , in which the neighbors of x excluding y are $\{x_1, x_2, x_3\}$ ($p = 3$) and the neighbors of y excluding x are $\{y_1, y_2, y_3, y_4\}$ ($q = 4$). We show the graph distance $d_G(x_2, y_3)$ between points x_2 and y_3 in green. By optimizing the expression given in Eq. (II.3), we arrive at the Earth Mover distance $W_1(x, y)$, which then allows us to calculate the ORC $\gamma(x, y)$ associated with the edge (x, y) using Eq. (II.2).

to y_j , which incurs a cost of $d_G(x_i, y_j)\gamma_{ij}$. We solve the following linear program with $p \times q$ variables and $p + q$ constraints:

$$W_1(x, y) = \min_{\{\gamma_{ij}\}} \sum_{i=1}^p \sum_{j=1}^q d_G(x_i, y_j)\gamma_{ij}, \quad (\text{II.3})$$

$$\forall j : \sum_{i=1}^p \gamma_{ij} = 1/q, \quad (\text{II.4})$$

$$\forall i : \sum_{j=1}^q \gamma_{ij} = 1/p, \quad (\text{II.5})$$

$$\forall i, j : \gamma_{ij} \geq 0. \quad (\text{II.6})$$

As a demonstration, in Appendix A, we calculate $\gamma(x, y)$ in the graph illustrated in Fig. 1, assuming that all edges are unit-length. We note that the definition of $W_1(x, y)$ varies, e.g., in [62, 63], the summation above does include y as neighborhood of x (and vice versa). However, either definition is practically fine and does not lose the generality of our subsequent construction.

In general, a linear program does not admit a closed form solution and needs to be solved algorithmically. An open question in the field of optimization that has resisted progress for several decades is whether linear programming can be solved in strongly polynomial time. All known algorithms are either worst-case exponential (in the number of variables, for fixed dimension linear programming is strongly polynomial) or algebraic/numerical and thus depend on the bit complexity of the input [64, 65].

The particular category that our linear program computes $W_1(x, y)$ falls into is the structured *optimal transport* problem, for which there exist strongly polynomial algorithms. We give a brief survey of some of these and refer the reader to the references listed for more details.

1. Orlin's strongly polynomial time combinatorial exact algorithm that runs in $O(pq(p + q) \log(p + q))$ for finding the min-cost flow on an uncapacitated complete bipartite graph $K_{p,q}$ [66].
2. A recent breakthrough gives an $O((pq)^{1+o(1)})$ algorithm for optimal transport with polynomially bounded integral demands and supplies (into which we can easily transform our linear program, by scaling both demands and supplies by a factor of pq) [67].
3. When $p = q$, the 1-Wasserstein optimal transport problem becomes a linear assignment (matching) problem. To see this, rescale the variables by letting $\Gamma_{ij} = p \gamma_{ij}$. Then $\sum_{j=1}^p \Gamma_{ij} = 1$ and $\sum_{i=1}^p \Gamma_{ij} = 1$, so the matrix $\Gamma \in \mathbb{R}^{p \times p}$ is a square *doubly stochastic matrix* [68]. The objective II.3 becomes $\frac{1}{p} \sum_{i=1}^p \sum_{j=1}^p d_G(x_i, y_j) \Gamma_{ij}$ which is equivalent (up to a constant factor, in the context of a linear program) to $\sum_{i,j} d_G(x_i, y_j) \Gamma_{ij}$.

By the classic Birkhoff theorem [69], every doubly stochastic matrix can be expressed as a convex combination of permutation matrices (matrices with exactly one 1 in each row and column). Equivalently, the permutation matrices are precisely the vertices of the Birkhoff polytope, which contains all doubly stochastic matrices. We are to optimize a linear objective function over the set of all doubly stochastic matrices and since in any linear program, if an optimal solution exists and the optimum value is finite (which is the case for our problem since the Birkhoff polytope is compact), then at least one optimal solution lies at a vertex of the feasible polytope [64, 65]. Thus it suffices to find an optimal permutation matrix. In this case, an optimal transport plan sends all the mass at each vertex to exactly one other vertex, so the problem reduces to a balanced matching problem, solvable by the Hungarian algorithm. (However, the optimal value of the objective function $W_1(x, y)$ still depends on the cost structure and does not admit a closed-form expression [70].)

We note that while there are other approaches with better asymptotic running times, the Hungarian algorithm has a small constant in the big O and works well in practice with moderately sized instances, along with plentiful off-the-shelf implementations that are highly optimized, so the Hungarian algorithm remains the standard in many applications.

4. When the distances between the supply and demand nodes are *decomposable*, i.e., $d_{ij} = e_i + f_j$ or $d_{ij} = e_i + f_j + C$ (C is a constant), the solution is remarkably simple, as any feasible transport is optimal [16]. For instance, when G is a tree, since there is only one path from any x_i to any y_j : $(x_i, x), (x, y), (y, y_j)$, we always have $d_G(x_i, y_j) = d_G(x_i, x) + d_G(x, y) + d_G(y, y_j)$, and therefore we have

$$W_1(x, y) = \frac{1}{p} \sum_{i=1}^p d_G(x_i, x) + d_G(x, y) + \frac{1}{q} \sum_{j=1}^q d_G(y, y_j). \quad (\text{II.7})$$

The classical algorithm in this case just needs to perform the summation, which takes $\mathcal{O}(p+q)$ time.

As can be seen above, the complexity of the classical algorithms, and hence their complexities vary case by case, as linear programming in general is difficult and a closed-form solution does not exist. In this work, we pay particular attention to (1) when G forms a tree and (2) when $p = q$. In these cases, there are certain patterns in the solutions that we could exploit to construct the corresponding quantum algorithms. Before moving on to construct such algorithms, we summarize the main results in the following theorem, showing how our quantum algorithm is advantageous over the classical one.

Theorem II.1. *Provided the raw distances $d(x_i, x_j)$ between a pair (x_i, x_j) among N data points. Then:*

- When G is a tree, $W_1(x, y)$ can be estimated with accuracy ϵ using a quantum circuit of complexity $\mathcal{O}\left(\frac{1}{\epsilon} \log(N) \log^2\left(\frac{1}{\epsilon}\right) \kappa \log^2\left(\frac{\kappa}{\epsilon}\right) + \frac{1}{\epsilon} \log(pq)\right)$.
- When $p = q$, $W_1(x, y)$ can be estimated with accuracy ϵ using a quantum circuit of complexity

$$\mathcal{O}\left(\left(\log(N) \log^2\left(\frac{1}{\epsilon}\right) \kappa \log^2\left(\frac{\kappa}{\epsilon}\right) + \log(p \log p)\right) \frac{1}{\gamma} p \log\left(\frac{p}{\epsilon}\right) \left(\frac{1}{\epsilon}\right) \log^2\frac{1}{\epsilon}\right),$$

where in the above, $\kappa = \min_{i,j,q,k} \left\{ \frac{d_G(x_i, x_j)}{d_G(x_k, x_q)} \right\}$, and γ is a

randomized factor that could be of $\mathcal{O}(1)$ in the best case

and of $\mathcal{O}(\exp(p))$ in the worst case.

The complexity of classical algorithms for the case G being a tree and for the case $p = q$ is, respectively, $\mathcal{O}(p+q)$ and $\mathcal{O}(p^3)$. However, these complexities do not include the time required to compute the geodesic distances from the raw distances $d(\mathbf{x}_i, \mathbf{x}_j)$ between a pair $(\mathbf{x}_i, \mathbf{x}_j)$ among N data points. Based on [71], the time complexity for producing geodesic distances from the raw distances is $\mathcal{O}(N^3)$. So the total classical complexity for estimating ORC are $\mathcal{O}(N^3 + pq)$ (for graph G being a tree) and $\mathcal{O}(N^3 + p^3)$ (for $p = q$), respectively. Compared to the quantum complexities above, there is exponential speed-up in the total number of points N in both cases. Regarding p, q (for the first case where G is a tree), which controls the size of local neighborhood of two points x, y of interest, there is still exponential speedup in the first case (when G is a tree). However, in the second case, the degree of speedup depends on the factor γ . As γ could be of $\mathcal{O}(1)$ in the best case and of $\mathcal{O}(\exp p)$ in the worst case, the best possible quantum speedup is polynomial. We remark one thing that as p (and q) controls the size of local neighborhood of x (and y), in principle, it can be chosen to be $\mathcal{O}(1)$. Thus, the scaling on p is $\mathcal{O}(1)$ in all cases and therefore, our quantum algorithm can guarantee to provide significant speed-up with respect to N – the number of data points, which is typically large in reality.

III. QUANTUM ALGORITHM

Before describing our main quantum algorithm, we provide some preliminaries. Our subsequent proposal shall be utilizing the block-encoding and quantum singular value transformation (QSVT) framework [72]. This framework was built on the qubitization and quantum signal processing technique [73, 74]. In particular, it was shown in [72] that the block-encoding/QSVT framework can unify many known quantum algorithms, thus providing a universal language for this area, motivating many subsequent refinements [75–77]. A key component of the block-encoding/QSVT framework is the unitary block-encoding of some operator. Specifically, a unitary U is said to be an exact block-encoding of a matrix A (with operator norm $\|A\| \leq 1$) if $A = (\langle \mathbf{0} | \otimes \mathbb{I})U(\mathbb{I} \otimes |0\rangle)$. If $(\langle \mathbf{0} | \otimes \mathbb{I})U(\mathbb{I} \otimes |0\rangle) = \tilde{A}$ and $\|\tilde{A} - A\| \leq \epsilon$, then U is said to be an ϵ -approximated block-encoding of A . Given two unitary U_1, U_2 that block-encode A_1, A_2 , then there is an efficient procedure that can construct the block-encoding of many operators, including linear combination of A_1, A_2 , product of A_1, A_2 , tensor product $A_1 \otimes A_2$, etc. A fundamental result of the QSVT [72] is that, given a unitary U that block-encodes A , then the unitary block-encoding of $f(A)$ can be constructed efficiently, where $f(\cdot)$ is some computable function. We note that a more complete summary of block-encoding and related recipes can be found in the Appendix B.

Our quantum algorithm, described below, is a continuation of the proposal initiated in [60], where the Gaussian curvature was considered. An important ingredient to our subsequent discussion is the following lemma:

Lemma III.1 (Appendix D of [60]). *Provided the raw distances $d(\mathbf{x}_i, \mathbf{x}_j)$ between a pair $(\mathbf{x}_i, \mathbf{x}_j)$ among N data points, then the ϵ -approximated block-encoding of the following operator*

$$\frac{1}{\alpha} \sum_{i,j=1}^N |i-1\rangle \langle i-1| \otimes d_G^4(\mathbf{x}_i, \mathbf{x}_j) |j-1\rangle \langle j-1| \quad (\text{III.1})$$

can be obtained by a quantum circuit of depth:

$$\mathcal{O}\left(\log(N) \log^2\left(\frac{1}{\epsilon}\right)\right), \quad (\text{III.2})$$

where $\alpha \in \mathcal{O}(1)$ is a constant that generally depend on the data set.

Moreover, we point out the following result of [75] and [72]:

Lemma III.2 (Positive Power Exponent [72],[75]). *Given a block encoding of a positive matrix \mathcal{M}/γ such that*

$$\frac{\mathbb{I}}{\kappa_M} \leq \frac{\mathcal{M}}{\gamma} \leq \mathbb{I},$$

and let $c \in (0, 1)$, then we can implement an ϵ -approximated block encoding of $(\mathcal{M}/\gamma)^c/2$ in time complexity $\mathcal{O}(\kappa_M T_M \log^2(\frac{\kappa_M}{\epsilon}))$, where T_M is the complexity to obtain the block encoding of \mathcal{M}/γ .

A direct application of Lemma III.1 and the lemma above (with $c = \frac{1}{4}$) allows us to obtain the following lemma:

Lemma III.3. *The ϵ -approximated block-encoding of the following*

$$\frac{1}{\alpha^{1/4}} \sum_{i,j=1}^N |i-1\rangle \langle i-1| \otimes d_G(\mathbf{x}_i, \mathbf{x}_j) |j-1\rangle \langle j-1| \quad (\text{III.3})$$

can be obtained using a quantum circuit of depth:

$$\mathcal{O}\left(\log(N) \log^2\left(\frac{1}{\epsilon}\right) \kappa \log^2 \frac{\kappa}{\epsilon}\right), \quad (\text{III.4})$$

where κ is the condition number of the operator in Eqn. III.1, which can be seen to be $\kappa = \min_{i,j,q,k} \left\{ \frac{d_G(\mathbf{x}_i, \mathbf{x}_j)}{d_G(\mathbf{x}_k, \mathbf{x}_q)} \right\}$.

We have mentioned in the previous section that the closed-form solution to Eqn. II.3 generally does not exist. Therefore, in the following, we consider case by case and outline the corresponding quantum algorithm. For simplicity, we begin with the case when G is a tree, for which a closed-form solution does exist.

A. The case when \mathbf{G} is a tree

As mentioned, the solution to Eqn. II.3 in this case is given by:

$$W_1(x, y) = \frac{1}{p} \sum_{i=1}^p d_G(x_i, x) + d_G(x, y) + \frac{1}{q} \sum_{j=1}^q d_G(y, y_j). \quad (\text{III.5})$$

In Section II, we have used the notation $\mathcal{N}_x \setminus \{y\} \equiv \{x_1, x_2, \dots, x_p\}$ to denote the set of neighbor points of x . The key lemma III.1 uses \mathbf{x}_i to denote the i -th data point in the given data set. To make things more appropriate, without loss of generalization, we promote the following index interchange $x_i \leftrightarrow \mathbf{x}_i$. For simplicity, the set $\mathcal{N}_x \setminus \{y\} \equiv \{x_1, x_2, \dots, x_p\}$ is then labeled as:

$$\{x_1, x_2, \dots, x_p\} \equiv \{\mathbf{x}_1, \mathbf{x}_2, \dots, \mathbf{x}_p\}. \quad (\text{III.6})$$

In a similar manner, the set $\mathcal{N}_y \setminus \{x\} = \{y_1, y_2, \dots, y_q\}$ is labeled as:

$$\{y_1, y_2, \dots, y_q\} \equiv \{\mathbf{x}_{p+1}, \mathbf{x}_{p+2}, \dots, \mathbf{x}_{p+q}\}. \quad (\text{III.7})$$

In this convention, the indexes of x_i, y_i (for $1 \leq i \leq p$) are $i, p+i$, respectively. In particular, we set x to have index i_x and y to have index i_y . To estimate $W_1(x, y)$, we assume that the indexes of x and y are classically known,

as well as the neighbors of x and y , which are $\{i_1, i_2, \dots, i_p\}$ and $\{j_1, j_2, \dots, j_q\}$, respectively. Denote the index of x by i_x , we note that the block-encoded operator

$$\mathcal{D} \equiv \frac{1}{\alpha^{1/4}} \sum_{i=1}^N \sum_{j=1}^N |i-1\rangle \langle i-1| \otimes d_G(\mathbf{x}_i, \mathbf{x}_j) |j-1\rangle \langle j-1|$$

can be decomposed as:

$$\begin{aligned} & \frac{1}{\alpha^{1/4}} \sum_{\mathbf{x}_i, \mathbf{x}_j \notin \mathcal{N}_x \setminus y} |i-1\rangle \langle i-1| \otimes d_G(\mathbf{x}_i, \mathbf{x}_j) |j-1\rangle \langle j-1| + \\ & \frac{1}{\alpha^{1/4}} \sum_{\mathbf{x}_i \in \mathcal{N}_x \setminus y} |i_x-1\rangle \langle i_x-1| \otimes d_G(x, \mathbf{x}_i) |i-1\rangle \langle i-1|. \end{aligned} \quad (\text{III.8})$$

Let U_d denote the unitary block-encoding of the above operator. Provided the classical knowledge of indices $\{1, 2, 3, \dots, p\}$ and also of x , the following state can be prepared using a depth-1 circuit:

$$|\phi\rangle = \frac{1}{\sqrt{p+1}} |i_x-1\rangle \otimes \sum_{i=1}^p |i-1\rangle, \quad (\text{III.9})$$

using a quantum circuit of depth $\mathcal{O}(\log p)$ and $\mathcal{O}(1)$ ancilla, based on the state preparation method [78, 79]. If we take the unitary U_d and apply it to the state $|\mathbf{0}\rangle |\phi\rangle$, according to Definition B.1, we obtain the state:

$$\begin{aligned} U_d |\mathbf{0}\rangle |\phi\rangle &= |\mathbf{0}\rangle \left(\frac{1}{\alpha^{1/4}} \sum_{\mathbf{x}_i, \mathbf{x}_j \notin \mathcal{N}_x \setminus y} |i-1\rangle \langle i-1| \otimes d_G(\mathbf{x}_i, \mathbf{x}_j) |j-1\rangle \langle j-1| + \right. \\ & \left. \frac{1}{\alpha^{1/4}} \sum_{\mathbf{x}_i \in \mathcal{N}_x \setminus y} |i_x-1\rangle \langle i_x-1| \otimes d_G(x, \mathbf{x}_i) |i-1\rangle \langle i-1| \right) \frac{1}{\sqrt{p+1}} \sum_{i=1}^p |i_x-1\rangle |i-1\rangle + |\text{Garbage}\rangle, \end{aligned} \quad (\text{III.10})$$

where $|\text{Garbage}\rangle$ is orthogonal to the first part. It can be seen that the above state is equivalent to:

$$\frac{1}{\alpha^{1/4} \sqrt{p+1}} |\mathbf{0}\rangle \sum_{i=1}^p d_G(x, \mathbf{x}_i) |i_x-1\rangle |i-1\rangle + |\text{Garbage}\rangle. \quad (\text{III.11})$$

Next, we consider the overlaps between the above state and $|\mathbf{0}\rangle |\phi\rangle$ again:

$$\begin{aligned} & \langle \mathbf{0} | \langle \phi | \cdot \left(\frac{1}{\alpha^{1/4} \sqrt{p+1}} |\mathbf{0}\rangle \sum_{i=1}^p d_G(x, \mathbf{x}_i) |i_x-1\rangle |i-1\rangle + |\text{Garbage}\rangle \right) \\ &= \left(\frac{1}{\sqrt{p+1}} \sum_{i=1}^p \langle i_x-1 | \langle i-1 | \right) \times \left(\frac{1}{\alpha^{1/4} \sqrt{p+1}} |\mathbf{0}\rangle \sum_{i=1}^p d_G(x, \mathbf{x}_i) |i_x-1\rangle |i-1\rangle + |\text{Garbage}\rangle \right) \\ &= \frac{1}{\alpha^{1/4} (p+1)} \sum_{i=1}^p d_G(x, \mathbf{x}_i) = \frac{1}{\alpha^{1/4} (p+1)} \sum_{i=1}^p d_G(x, x_i). \end{aligned} \quad (\text{III.12})$$

These overlaps can be estimated via standard methods, such as the Hadamard test, SWAP test, or amplitude estimation. The value of the desired quantity $\frac{1}{p} \sum_{i=1}^p d_G(x_i, x)$ can be derived from the above estimation accordingly, e.g., by multiplying $\frac{1}{\alpha^{1/4}(p+1)} \sum_{i=1}^p d_G(x, x_i)$ with $\frac{\alpha^{1/4}(p+1)}{p}$.

Repeating the above procedure but interchanging $x \leftrightarrow y, p \leftrightarrow q$, and $\{x_1, x_2, \dots, x_p\} \leftrightarrow \{y_1, y_2, \dots, y_q\}$ can allow us to estimate the summation $\frac{1}{q} \sum_{j=1}^q d_G(y, y_j)$. The value $d_G(x, y)$ is, in fact, a special case of the above estimation, as we just need to set a fixed value of index x, y . Instead of preparing $|\phi\rangle$ as above, we just need to prepare the state $|i_x - 1\rangle |i_y - 1\rangle$ and execute the same procedure. From the value of $W_1(x, y)$ and also $d_G(x, y)$, the estimation for the Ollivier-Rici curvature is straightforward as $\kappa(x, y) = 1 - \frac{W_1(x, y)}{d_G(x, y)}$.

Complexity. To analyze the total quantum circuit depth for this part, we summarize the above procedure in the following steps.

- **Step 1.** Obtain the ϵ -approximated unitary block-encoding U_d of

$$\frac{1}{\alpha^{1/4}} \sum_{i=1}^N \sum_{j=1}^N |i-1\rangle \langle i-1| \otimes d_G(\mathbf{x}_i, \mathbf{x}_j) |j-1\rangle \langle j-1| \quad (\text{III.13})$$

via Lemma III.3, which involves a quantum circuit of depth:

$$\mathcal{O} \left(\log(N) \log^2 \left(\frac{1}{\epsilon} \right) \kappa \log^2 \frac{\kappa}{\epsilon} \right). \quad (\text{III.14})$$

- **Step 2.** The state $|\phi\rangle$ (and hence, $|\mathbf{0}\rangle|\phi\rangle$) can be prepared using a circuit of depth $\mathcal{O}(\log p)$. Therefore, the quantum circuit depth that prepares the state $U_d |\mathbf{0}\rangle|\phi\rangle$ is:

$$\mathcal{O} \left(\log(N) \log^2 \left(\frac{1}{\epsilon} \right) \kappa \log^2 \left(\frac{\kappa}{\epsilon} \right) + \log p \right). \quad (\text{III.15})$$

- **Step 3.** The overlap estimation with a precision ϵ incurs a total complexity

$$\mathcal{O} \left(\frac{1}{\epsilon} \log(N) \log^2 \left(\frac{1}{\epsilon} \right) \kappa \log^2 \left(\frac{\kappa}{\epsilon} \right) + \frac{1}{\epsilon} \log p \right). \quad (\text{III.16})$$

For completeness, we recall that $\kappa = \min_{i,j,q,k} \left\{ \frac{d_G(\mathbf{x}_i, \mathbf{x}_j)}{d_G(\mathbf{x}_k, \mathbf{x}_q)} \right\}$.

- **Step 4.** Finally repeat the above step with the interchange $x \leftrightarrow y, p \leftrightarrow q, \{x_1, x_2, \dots, x_p\} \leftrightarrow \{y_1, y_2, \dots, y_q\}$, leads to the same complexity as above, but with p replaced by q :

$$\mathcal{O} \left(\frac{1}{\epsilon} \log(N) \log^2 \left(\frac{1}{\epsilon} \right) \kappa \log^2 \left(\frac{\kappa}{\epsilon} \right) + \frac{1}{\epsilon} \log q \right). \quad (\text{III.17})$$

Hence, the total complexity is:

$$\mathcal{O} \left(\frac{1}{\epsilon} \log(N) \log^2 \left(\frac{1}{\epsilon} \right) \kappa \log^2 \left(\frac{\kappa}{\epsilon} \right) + \frac{1}{\epsilon} \log(pq) \right). \quad (\text{III.18})$$

B. The case when $p = q$

This is considerably harder than in the previous case, as we have discussed in Section II. Although the Hungarian algorithm [70] can solve this case exactly in polynomial time, below, we shall attempt to derive a quantum algorithm running in linear time, at the cost of achieving the approximation. We first recall that the reasoning of [70] results in the matrix $\gamma \equiv [\gamma_{ij}]_{p \times p}$ being a permutation matrix multiplied by a factor of $\frac{1}{p}$. Given that the Earth Mover (1-Wasserstein) distance $W_1(x, y)$ is defined as

$$W_1(x, y) = \min_{\gamma_{ij}} \sum_{i=1}^p \sum_{j=1}^q \frac{1}{p} d_G(x_i, y_j) \gamma'_{ij}. \quad (\text{III.19})$$

where $\gamma' \equiv [\gamma'_{ij}]$ is the permutation matrix. Then if we organize $\{d_G(x_i, y_j)\}_{i,j=1}^p$ as a $p \times p$ matrix, and define $d_G \equiv [d_G(x_i, y_j)]_{i,j=1}^p \equiv [d_{ij}]_{i,j=1}^p$ be the $p \times p$ matrix with entries being the geodesic distances as indicated. The minimization problem can then be translated into the following problem:

For each column index i , find an element j so that their summation $\sum_{i=1}^p d_{\pi(i),i}$ is minimized. In other words, we need to find the minimum value of $\{d_{i_11} + d_{i_22} + \dots + d_{i_pp}\}_{i_1 \neq i_2 \neq \dots \neq i_p}^p$.

How do we compute the above sum and minimize over all possible permutations? Our algorithm is built on the following observation. Suppose, for now, that $p = 3$. Then we have:

$$d_G = \begin{pmatrix} d_{11} & d_{12} & d_{13} \\ d_{21} & d_{22} & d_{23} \\ d_{31} & d_{32} & d_{33} \end{pmatrix}. \quad (\text{III.20})$$

Consider the following 9×9 diagonal matrix:

$$D_G = \text{diag}(d_{11}, d_{21}, d_{31}, d_{12}, d_{22}, d_{32}, d_{13}, d_{23}, d_{33}). \quad (\text{III.21})$$

We define three blocks D_1, D_2, D_3 as follows:

$$\begin{aligned} D_1 &= \text{diag}(d_{11}, d_{21}, d_{31}), \\ D_2 &= \text{diag}(d_{12}, d_{22}, d_{32}), \\ D_3 &= \text{diag}(d_{13}, d_{23}, d_{33}). \end{aligned} \quad (\text{III.22})$$

Next, we consider the top-left corner sub-matrix of dimension 9×9 , denoted by $[\cdot]_{9 \times 9}$ of:

$$\begin{aligned} [D_1 \otimes \mathbb{I}_9]_{9 \times 9} &= \\ &\text{diag}(d_{11}, d_{11}, d_{11}, d_{11}, d_{11}, d_{11}, d_{11}, d_{11}, d_{11}), \\ [\mathbb{I}_3 \otimes D_2 \otimes \mathbb{I}_3]_{9 \times 9} &= \\ &\text{diag}(d_{12}, d_{12}, d_{12}, d_{22}, d_{22}, d_{22}, d_{32}, d_{32}, d_{32}), \\ [\mathbb{I}_9 \otimes D_3]_{9 \times 9} &= \\ &\text{diag}(d_{13}, d_{23}, d_{33}, d_{13}, d_{23}, d_{33}, d_{13}, d_{23}, d_{33}). \end{aligned} \quad (\text{III.23})$$

Their summation is as follows (again, we pay attention to the top-left corner of dimension 9×9):

$$\begin{aligned} [D_1 \otimes \mathbb{I}_9 + \mathbb{I}_3 \otimes D_2 \otimes \mathbb{I}_3 + \mathbb{I}_9 \otimes D_3]_{9 \times 9} &= \\ &\text{diag}(d_{11} + d_{12} + d_{13}, d_{11} + d_{12} + d_{23}, d_{11} + d_{12} + d_{33}, \\ &d_{11} + d_{22} + d_{13}, d_{11} + d_{22} + d_{23}, d_{11} + d_{22} + d_{33}, \\ &d_{11} + d_{32} + d_{13}, d_{11} + d_{32} + d_{23}, d_{11} + d_{32} + d_{33}). \end{aligned} \quad (\text{III.24})$$

We recall that the above operator is the top-left corner submatrix of $D_1 \otimes \mathbb{I}_9 + \mathbb{I}_3 \otimes D_2 \otimes \mathbb{I}_3 + \mathbb{I}_9 \otimes D_3$ with dimension 9×9 . If we pay attention to the next block submatrix of the same dimension 9×9 , e.g., the submatrix whose row and column indices run from $9 \rightarrow 18$ of matrix $D_1 \otimes \mathbb{I}_9 + \mathbb{I}_3 \otimes D_2 \otimes \mathbb{I}_3 + \mathbb{I}_9 \otimes D_3$, then the structure is same as above but the entries d_{11} is replaced by d_{12} . In a similar manner, the next submatrix of dimension 9×9 , or the submatrix whose row and column indexes run from $18 \rightarrow 27$ of $D_1 \otimes \mathbb{I}_9 + \mathbb{I}_3 \otimes D_2 \otimes \mathbb{I}_3 + \mathbb{I}_9 \otimes D_3$ has the diagonal entries being similar as above, but d_{11} is replaced with d_{13} . What we can conclude from this observation is that

The matrix $D_1 \otimes \mathbb{I}_9 + \mathbb{I}_3 \otimes D_2 \otimes \mathbb{I}_3 + \mathbb{I}_9 \otimes D_3$ has the entries $\{(d_{i1} + d_{j2} + d_{k3})\}_{i,j,k=1}^3$ in the diagonal.

By generalizing the above procedure to arbitrary value of p , we then have the following property, stated as a lemma for subsequent reference:

Lemma III.4. Let $d_G(x_i, y_j)$ be the geodesic distances between the points x_i and y_j from the given dataset. Define $d_G \equiv [d_G(x_i, y_j)]_{i,j=1}^p \equiv [d_{ij}]_{i,j=1}^p$ as the corresponding geodesic distance matrix of those points belonging to the neighbor of two points x, y of consideration.

Let D_G be the matrix of dimension $p \times p$ defined as $D_G \equiv \sum_{i,j=1}^p d_{ji} |i\rangle \langle i| \otimes |j\rangle \langle j|$ which contains the geodesic distances on the diagonal. Define p block submatrices as $D_i = \bigoplus_{j=1}^p d_{ji} |j\rangle \langle j|$ for $i = 1, 2, \dots, p$. Then it holds that

$$D_P \equiv D_1 \otimes \mathbb{I}_p^{\otimes p-1} + \mathbb{I}_p \otimes D_2 \otimes \mathbb{I}_p^{\otimes p-2} + \dots + \mathbb{I}_p^{\otimes p-1} \otimes D_p$$

is diagonal and contains $\{d_{i_11} + d_{i_22} + \dots + d_{i_p p}\}_{i_1, i_2, \dots, i_p=1}^p$ in the diagonal.

However, we need to restrict to the cases where the indices i_k 's are all different. Namely, for the case

($p = q$) the objective reduces to finding the minimum of $\{\sum_{i=1}^p d_{\pi(i),i}\}_{i=1}^p$. The permutation requires that only a subset of $\{d_{i_11} + d_{i_22} + \dots + d_{i_p p}\}_{i_1, i_2, \dots, i_p=1}^p$ is of interest. In order to filter out those elements that correspond to the permutation of the indices, we shall construct a projector Π , see Eq. (III.26) below, that achieves this goal. Let us first point out the following property. Within the matrix \mathcal{D}_P , which has size $p^p \times p^p$, the entry having value $d_{i_11} + d_{i_22} + \dots + d_{i_p p}$ would have the location index (along the diagonal) as:

$$k = (i_1 - 1)p^{p-1} + (i_2 - 1)p^{p-2} + \dots + i_p. \quad (\text{III.25})$$

Because the summation $\sum_{i=1}^p d_{\pi(i),i}$ only contains the permutation for all i , it implies that the indices i_1, i_2, \dots, i_p in the summation $d_{i_11} + d_{i_22} + \dots + d_{i_p p}$ must be different (no pair of indices having the same value). So, among all the diagonal entries, only those entries with the index $k = (i_1 - 1)p^{p-1} + (i_2 - 1)p^{p-2} + \dots + i_p$ with $i_1 \neq i_2 \neq \dots \neq i_p$ are of interest. To obtain these elements, we consider the projector

$$\Pi = \sum_{k: i_1 \neq i_2 \neq \dots \neq i_p} |k\rangle \langle k|, \quad (\text{III.26})$$

whose construction is shown below right above Lemma III.5. The product of this projector with \mathcal{D}_P contains those $\{\sum_{i=1}^p d_{\pi(i),i}\}_{i=1}^p$ of interest.

Our problem then is to find the minimum diagonal entry of the matrix $\Pi \mathcal{D}_P$. This is trivially equivalent to the minimum (nonzero) eigenvalue of the matrix. However, before proceeding with the eigenvalue solver, we describe a procedure for constructing the block-encoding of D_G , as well as that of $\mathcal{D}_P, \Pi \mathcal{D}_P$.

Block encoding of D_G . First, from Lemma III.3, we have the block-encoding of

$$\frac{1}{\alpha^{1/4}} \sum_{i=1}^N \sum_{j=1}^N |i-1\rangle \langle i-1| \otimes d_G(\mathbf{x}_i, \mathbf{x}_j) |j-1\rangle \langle j-1|, \quad (\text{III.27})$$

which contains the geodesic distances between *every pair* of points in the given data. Our goal now is to first obtain the (block-encoding of) operator D_G that appears in the lemma above, which only includes certain data points of interest, before finding the minimum of $D_1 \otimes \mathbb{I}_p^{\otimes p} + \mathbb{I}_p \otimes D_2 \otimes \mathbb{I}_p^{\otimes p-1} + \dots + \mathbb{I}_p^{\otimes p} \otimes D_p$.

In the previous section, we have defined the classical indexes $\{\mathbf{x}_1, \mathbf{x}_2, \dots, \mathbf{x}_p\}$ and $\{\mathbf{x}_{p+1}, \mathbf{x}_{p+2}, \dots, \mathbf{x}_{p+q}\}$ of the neighbors of x and y , respectively. Now we define the permutation operator U_p of dimension $N^2 \times N^2$ that acts as follows:

$$\begin{cases} U_p |i\rangle |j\rangle \leftrightarrow |i\rangle |j-p\rangle \\ \text{arbitrary for the remaining basis} \end{cases} \quad (\text{III.28})$$

An arbitrary permutation of a given dimension can be constructed with polylogarithmic resources [80, 81].

That being said, the unitary U_p can be constructed using a quantum circuit of depth $\mathcal{O}(\log(N \log N))$. However, we note that we are only limiting ourselves to the space spanned by those neighbors of x and y (with the corresponding indexes $\{1, 2, 3, \dots, p, p+1, p+2, \dots, p+p\}$, which is effectively of dimension p^2). Thus, the unitary U_p can be effectively realized with a circuit of depth $\mathcal{O}(\log(p \log p))$.

Given the unitary U_p , according to Def. B.1, it block-encodes itself. Then we use Lemma B.1 to construct the block-encoding of:

$$\begin{aligned} U_p \frac{1}{\alpha^{1/4}} \sum_{i=1}^N \sum_{j=1}^N & |i-1\rangle \langle i-1| \otimes d_G(\mathbf{x}_i, \mathbf{x}_j) |j-1\rangle \langle j-1| U_p^\dagger \\ &= \frac{1}{\alpha^{1/4}} \sum_{i,j=1}^p d_G(\mathbf{x}_i, \mathbf{y}_j) |i-1\rangle \langle i-1| \otimes |j-1\rangle \langle j-1| + (\dots), \\ &= \frac{1}{\alpha^{1/4}} \sum_{i,j=1}^p d_{ij} |i-1\rangle \langle i-1| \otimes |j-1\rangle \langle j-1| + (\dots), \end{aligned} \quad (\text{III.29})$$

where (\dots) refers to the unwanted part (which contains the distance between other pairs), and we only pay attention to the top-left submatrix of size $p \times p$.

Next, we define the SWAP operator that performs the swapping between two sub-systems of dimension p , e.g., $|i-1\rangle \langle i-1| \leftrightarrow |j-1\rangle \langle j-1|$. This operator can be realized with a circuit of depth $\mathcal{O}(\log p)$ [80] (in fact, they are a specific kind of permutation). We then use Lemma B.1 to construct the block-encoding of:

$$\begin{aligned} \text{SWAP} \cdot \frac{1}{\alpha^{1/4}} \sum_{i=1}^p \sum_{j=1}^p d_{ij} & |i-1\rangle \langle i-1| \otimes |j-1\rangle \langle j-1| \text{SWAP}^\dagger \\ &= \frac{1}{\alpha^{1/4}} \sum_{i=1}^p \sum_{j=1}^p d_{ij} |j-1\rangle \langle j-1| \otimes |i-1\rangle \langle i-1|. \end{aligned} \quad (\text{III.30})$$

Up to the scaling factor $\alpha^{1/4}$, the above operator contains the geodesic distances $\{d_{ij} \equiv d_G(\mathbf{x}_i, \mathbf{y}_j)\}$ on the diagonal. Defining the above operator multiplied by $\alpha^{1/4}$ as D_G , therefore, we have obtained the block-encoding of $D_G/\alpha^{1/4}$.

Block-encoding of \mathcal{D}_P . We now discuss how to construct the block encoding of $\mathcal{D}_P \equiv D_1 \otimes \mathbb{I}_p^{\otimes p} + \mathbb{I}_p \otimes D_2 \otimes \mathbb{I}_p^{\otimes p-1} + \dots + \mathbb{I}_p^{\otimes p} \otimes D_p$. First, we note that $D_G = \sum_{i=1}^p |i\rangle \langle i| \otimes D_i$. Next, we define p different permutations U_1, \dots, U_p that act as follows: for any $i = 1, 2, \dots, p$,

$$U_i |i\rangle \leftrightarrow |0\rangle \quad (\text{III.31})$$

and the remaining bases are permuted arbitrarily (for all i). Based on [80, 81], these unitaries can be constructed using circuits of depth $\mathcal{O}(\log(p \log p))$. Next, for each i , we use U_i which block-encodes itself, and Lemma B.1 to construct the block-encoding of:

$$U_i \frac{D_G}{\alpha^{1/4}} U_i^\dagger = U_i \frac{\sum_{i=1}^p |i\rangle \langle i| \otimes D_i}{\alpha^{1/4}} U_i^\dagger \quad (\text{III.32})$$

$$= \frac{1}{\alpha^{1/4}} |0\rangle \langle 0| \otimes D_i + (\dots), \quad (\text{III.33})$$

where (\dots) refers to the unwanted part. It can be seen that, from the Definition B.1, the above operator is exactly the block-encoding of $\frac{1}{\alpha^{1/4}} D_i$. Repeating the same procedure for different permutations U_i 's, we obtain the block-encoding of all $\frac{1}{\alpha^{1/4}} D_i$ for $i = 1, 2, \dots, p$.

The remaining task for constructing \mathcal{D}_P is straightforward as follows. As the block encoding for the identity matrix of arbitrary dimension can be constructed easily (see Def. B.1), we can employ Lemma B.2 to construct the block-encoding of the following operators

$$\frac{1}{\alpha^{1/4}} D_1 \otimes \mathbb{I}_p^{\otimes p-1}, \frac{1}{\alpha^{1/4}} \mathbb{I}_p \otimes D_2 \otimes \mathbb{I}_p^{\otimes p-2}, \dots, \frac{1}{\alpha^{1/4}} \mathbb{I}_p^{\otimes p-1} \otimes D_p. \quad (\text{III.34})$$

Then we use Lemma B.3 to construct the block encoding of their linear combination,

$$\frac{1}{p} \left(\frac{1}{\alpha^{1/4}} D_1 \otimes \mathbb{I}_p^{\otimes p-1} + \frac{1}{\alpha^{1/4}} \mathbb{I}_p \otimes D_2 \otimes \mathbb{I}_p^{\otimes p-2} + \dots + \frac{1}{\alpha^{1/4}} \mathbb{I}_p^{\otimes p-1} \otimes D_p \right) \quad (\text{III.35})$$

$$= \frac{1}{p\alpha^{1/4}} (D_1 \otimes \mathbb{I}_p^{\otimes p-1} + \mathbb{I}_p \otimes D_2 \otimes \mathbb{I}_p^{\otimes p-2} + \dots + \mathbb{I}_p^{\otimes p-1} \otimes D_p) = \frac{1}{p\alpha^{1/4}} \mathcal{D}_P. \quad (\text{III.36})$$

Block-encoding of Π . Next, we show how to obtain the block-encoding of the projector Π in Eq. (III.26) that allows us to restrict the indices to the permutations only, as remarked earlier. We first consider the state $\frac{1}{\sqrt{p!}} \sum_{k: i_1 \neq i_2 \neq \dots \neq i_p} |k\rangle$, which can be prepared using any of the state preparation methods in [79, 82–84]. These

methods generally have circuit complexity $\mathcal{O}(\log(p!))$. However, the method in [79] would require $\mathcal{O}(p!)$ ancilla qubit, meanwhile the methods in [82, 83] requires $\mathcal{O}(1)$ ancilla qubits; see e.g., Theorem 1 of [82]. In practice the value of $p = \mathcal{O}(1)$, therefore practically either of these methods can be used. However, we prefer the methods in [82, 83] as it requires less ancilla qubits.

Given the preparation of such the state, then we append the ancilla initialized in $|0\rangle^{\otimes \log p^p}$, and use CNOT gates to transform $\frac{1}{\sqrt{p!}} \sum_{k:i_1 \neq i_2 \neq \dots \neq i_p} |k\rangle |0\rangle^{\otimes \log p^p}$ to $\frac{1}{\sqrt{p!}} \sum_{k:i_1 \neq i_2 \neq \dots \neq i_p} |k\rangle |k\rangle$. Tracing out either of these register yields the normalized projector $\frac{1}{p!} \Pi$, which can be block-encoded via the following lemma:

Lemma III.5 (Block encoding of density matrix, see e.g. [72]). *Let $\rho = \text{Tr}_A |\Phi\rangle\langle\Phi|$, where $\rho \in \mathbb{H}_B$ and $|\Phi\rangle \in \mathbb{H}_A \otimes \mathbb{H}_B$. Given a unitary U that prepares $|\Phi\rangle$ from $|\mathbf{0}\rangle_A \otimes |\mathbf{0}\rangle_B$, there exists a highly efficient procedure that constructs an exact unitary block encoding of ρ using U and U^\dagger once each.*

Block-encoding of $\Pi\mathcal{D}_P$. From the block-encoding of $\frac{1}{p!} \Pi$ and of $\frac{1}{p\alpha^{1/4}} \mathcal{D}_P$, we can use Lemma B.1 to construct the block-encoding of $\frac{1}{p!p\alpha^{1/4}} \Pi\mathcal{D}_P$.

Finding the Earth Mover distance. Earlier, we have mentioned that the operator $\Pi\mathcal{D}_P$ contains the summations $\{\sum_{i=1}^p d_{\pi(i),i}\}_{i=1}^p$ of interest along the diagonal. It can be seen that for a diagonal matrix, the minimum entry along the diagonal is also the minimum eigenvalue. Therefore, our challenge now is to find the minimum eigenvalue of this block-encoded operator $\frac{1}{(p+1)!\alpha^{1/4}} \Pi\mathcal{D}_P$, which contains the desired minimum value of the Earth Mover distance $W_1(x, y)$ (up to a scaling). To this end, we point out the following result of [76, 77], which is based on the classical power method for finding the largest eigenvalues/eigenvectors:

Lemma III.6. *Let $A \in \mathbb{R}^{n \times n}$ be a Hermitian matrix of operator norm $\|A\|_{\text{operator}} \leq 1$. Let U_A be the block-encoding of A with circuit complexity T_A . Then its largest eigenvalue ψ_{\max} can be estimated up to an additive error ϵ using a quantum circuit of depth*

$$\mathcal{O}\left(T_A\left(\frac{1}{\Delta\gamma\epsilon}\right) \log\left(\frac{n}{\epsilon}\right) \log\left(\frac{1}{\epsilon}\right)\right),$$

where Δ is the gap between the largest and the second largest eigenvalue. γ is defined as $|\langle\psi_0, \psi_{\max}\rangle|$ where $|\psi_{\max}\rangle$ is the eigenstate corresponding to the largest eigenvalue, and $|\psi_0\rangle$ is some randomly initialized state.

While the above lemma aims at finding the largest eigenvalues/eigenvectors, it can be adapted to deal with the minimum ones by considering the matrix A' to be the inverse of A or the pseudoinverse of A if A is singular. In either case, the maximum nonzero eigenvalue of A' is equal to $\frac{1}{\psi_{\min}}$. An estimation of the largest eigenvalue of A' can thus be used to infer the minimum eigenvalue ψ_{\min} of A . The block-encoding of $\frac{A^{-1}}{\kappa_A}$ (where κ_A is the condition number of A) can be obtained from A by using matrix inversion technique of [30], or QSVT with a proper polynomial approximation to A^{-1} , e.g., see Corollary 67 in [72] and the discussion below such the corollary. As the inversion incurs a circuit complexity by $\mathcal{O}(\kappa_A \log \frac{1}{\epsilon})$,

so the total complexity for using the above lemma to find the minimum eigenvalue of A is

$$\mathcal{O}\left(T_A \kappa_A \left(\frac{1}{\Delta\gamma\epsilon}\right) \log\left(\frac{n}{\epsilon}\right) \log^2\left(\frac{1}{\epsilon}\right)\right).$$

The application of the above discussion to our context is straightforward to estimate:

$$\min \frac{1}{p!p\alpha^{1/4}} \left\{ \sum_{i=1}^p d_{\pi(i),i} \right\}_{i=1}^p \equiv \frac{W_1(x, y)}{p!\alpha^{1/4}}. \quad (\text{III.37})$$

from which the value of $W_1(x, y)$ can be inferred by multiplying such estimation with $p!\alpha^{1/4}$.

Complexity. To analyze the complexity, we recapitulate the algorithm above as follows.

- **Step 1.** Obtain the block-encoding of

$$\frac{1}{\alpha^{1/4}} \sum_{i,j=1}^N |i-1\rangle\langle i-1| \otimes d_G(\mathbf{x}_i, \mathbf{x}_j) |j-1\rangle\langle j-1| \quad (\text{III.38})$$

via Lemma III.3, which involves a quantum circuit of depth:

$$\mathcal{O}\left(\log(N) \log^2\left(\frac{1}{\epsilon}\right) \kappa \log^2\frac{\kappa}{\epsilon}\right). \quad (\text{III.39})$$

- **Step 2.** From the block-encoding of the above operator, construct the block-encoding of

$$\frac{1}{\alpha^{1/4}} \sum_{m,k=1}^p d_{mk} |m-1\rangle\langle m-1| \otimes |k-1\rangle\langle k-1| + (\dots),$$

which uses further a permutation operator and a SWAP operator of dimension $p \times p$, with circuit depth $\mathcal{O}(\log(p \log p))$. So the total complexity is:

$$\mathcal{O}\left(\log(N) \log^2\left(\frac{1}{\epsilon}\right) \kappa \log^2\frac{\kappa}{\epsilon} + \log(p \log p)\right). \quad (\text{III.40})$$

- **Step 3.** Use permutation operator of dimension $p \times p$ again to construct the block-encoding of $\frac{D_i}{\alpha^{1/4}}$ for all $i = 1, 2, \dots, p$. The total complexity at this point is

$$\mathcal{O}\left(\log(N) \log^2\left(\frac{1}{\epsilon}\right) \kappa \log^2\frac{\kappa}{\epsilon} + \log(p \log p)\right). \quad (\text{III.41})$$

- **Step 4.** Use Lemma B.3 to construct the block-encoding of

$$A \equiv \frac{(D_1 \otimes \mathbb{I}_p^{\otimes p-1} + \mathbb{I}_p \otimes D_2 \otimes \mathbb{I}_p^{\otimes p-2} + \dots + \mathbb{I}_p^{\otimes p-1} \otimes D_p)}{p\alpha^{1/4}},$$

which incurs a total quantum circuit depth

$$\mathcal{O}\left(p \log(N) \log^2\left(\frac{1}{\epsilon}\right) \kappa \log^2\frac{\kappa}{\epsilon} + p \log(p \log p)\right). \quad (\text{III.42})$$

- **Step 5.** Use the modified version of Lemma III.6 with A being defined as above to find the minimum

$$\mathcal{O} \left(\left(\log(N) \log^2 \left(\frac{1}{\epsilon} \right) \kappa \log^2 \left(\frac{\kappa}{\epsilon} \right) + \log(p \log p) \right) p \log \left(\frac{p}{\epsilon} \right) \left(\frac{1}{\Delta \gamma \epsilon} \right) \log^2 \frac{1}{\epsilon} \right), \quad (\text{III.43})$$

where in this case Δ is defined as the gap between the smallest and second smallest eigenvalue of the operator A ; and we recall that $\kappa = \min_{i,j,q,k} \left\{ \frac{d_G(\mathbf{x}_i, \mathbf{x}_j)}{d_G(\mathbf{x}_k, \mathbf{x}_q)} \right\}$.

Discussion. As indicated above, the complexity depends on a parameter γ , which is defined as $|\langle \psi_0, \psi_{\min} \rangle|$ where $|\psi_0\rangle$ is the initially randomized vector, and $|\psi_{\min}\rangle$ is the eigenstate corresponding to the minimum eigenvalue of A above. As it involves a randomization, the value of γ also behaves probabilistically. If we are lucky to have large overlaps, then γ is of $\mathcal{O}(1)$. Otherwise, in the worst case scenario, γ can be exponentially small as the dimension of matrix, and thus the complexity could scale as $\mathcal{O}(p^p)$, which is exponential in p . Therefore, in order for our method maintains its efficiency, the value of p should be small, of order $\mathcal{O}(1)$. This can be achieved by choosing a small neighborhood around x and y .

Earlier, we have noted that our definition of Earth Mover distance does not include the point x, y , and that adding these points (according to [62, 63]) would not change the procedure as well as the complexity of our algorithm.

IV. CONCLUSION

In this work, we have constructed a quantum algorithm for estimating the Ollivier-Ricci curvature in two specific classes of problems, an important quantity with practical applications. Our work incorporated a wide range of methods, including optimal transport theory (specifically its discrete version), linear programming, and, notably, the block-encoding/QSVT framework introduced in [72]. By leveraging the recent result in [60], we are able to ob-

tain the block-encoding of an operator that contains the geodesic distances between data points as diagonal entries. From such a (block-encoded) operator, we showed that a series of QSVT techniques can be applied appropriately, resulting in the estimation of the Earth Mover (1-Wasserstein) distance $W_1(x, y)$ for two classes of the problem: (1) when G forms a tree and (2) the case $p = q$, i.e., number of the respective neighbors of two points on an edge (x, y) is the same. Estimating the Ollivier-Ricci curvature in these cases can be straightforwardly done by quantum methods. We then provide an analysis showing that our quantum algorithm admits logarithmic running time in the number of data points, and also the (local) size of the neighborhood of interest. Thus, our quantum algorithm offers an exponential speedup compared to the classical algorithm. Our result has strongly highlighted the potential of quantum computation for geometrical data analysis, adding another example to our previous attempt [60]. What other problems in which our technique can be proved useful is thus of high interest. For example, the arbitrary case of the Ollivier-Ricci curvature remains open and is left for future exploration.

ACKNOWLEDGEMENTS

This work was supported by the U.S. Department of Energy, Office of Science, National Quantum Information Science Research Centers, Co-design Center for Quantum Advantage (C2QA) under Contract No. DE-SC0012704. N.A.N. and T.-C.W also acknowledge support from the Center for Distributed Quantum Processing at Stony Brook University. N.A.N. thanks the hospitality of Harvard University where he has an academic visit during the completion of this project.

- [1] Charles Fefferman, Sanjoy Mitter, and Hariharan Narayanan. Testing the manifold hypothesis. *Journal of the American Mathematical Society*, 29(4):983–1049, 2016.
- [2] Alexander N Gorban and Ivan Yu Tyukin. Blessing of dimensionality: mathematical foundations of the statistical physics of data. *Philosophical Transactions of the Royal Society A: Mathematical, Physical and Engineering Sciences*, 376(2118):20170237, 2018.
- [3] Bradley CA Brown, Anthony L Caterini, Brendan Leigh Ross, Jesse C Cresswell, and Gabriel Loaiza-Ganem. Verifying the union of manifolds hypothesis for image data. *arXiv preprint arXiv:2207.02862*, 2022.
- [4] Dagmar Sternad. It’s not (only) the mean that matters: variability, noise and exploration in skill learning. *Current opinion in behavioral sciences*, 20:183–195, 2018.

[5] Laurent Amsaleg, Oussama Chelly, Teddy Furon, Stéphane Girard, Michael E Houle, Ken-ichi Kawarabayashi, and Michael Nett. Estimating local intrinsic dimensionality. In *Proceedings of the 21th ACM SIGKDD International Conference on Knowledge Discovery and Data Mining*, pages 29–38, 2015.

[6] David Eppstein, Michael S Paterson, and F Frances Yao. On nearest-neighbor graphs. *Discrete & Computational Geometry*, 17(3):263–282, 1997.

[7] John M Lee. *Riemannian manifolds: an introduction to curvature*, volume 176. Springer Science & Business Media, 2006.

[8] Karish Grover, Geoffrey J Gordon, and Christos Faloutsos. Curvgad: Leveraging curvature for enhanced graph anomaly detection. *arXiv preprint arXiv:2502.08605*, 2025.

[9] Romeil S Sandhu, Tryphon T Georgiou, and Allen R Tannenbaum. Ricci curvature: An economic indicator for market fragility and systemic risk. *Science advances*, 2(5):e1501495, 2016.

[10] Areejit Samal, Hirdesh K Pharasi, Sarath Jyotsna Ramaia, Harish Kannan, Emil Saucan, Jürgen Jost, and Anirban Chakraborti. Network geometry and market instability. *Royal Society open science*, 8(2):201734, 2021.

[11] Vladimir Boginski, Sergiy Butenko, and Panos M Pardalos. Mining market data: A network approach. *Computers & Operations Research*, 33(11):3171–3184, 2006.

[12] K Tse Chi, Jing Liu, and Francis CM Lau. A network perspective of the stock market. *Journal of Empirical Finance*, 17(4):659–667, 2010.

[13] Yann Ollivier. Ricci curvature of metric spaces. *Comptes Rendus Mathématique*, 345(11):643–646, 2007.

[14] Yann Ollivier. Ricci curvature of markov chains on metric spaces. *Journal of Functional Analysis*, 256(3):810–864, 2009.

[15] Joaquin Sanchez Garcia and Sebastian Gherghe. On the ollivier-ricci curvature as fragility indicator of the stock markets, 2024.

[16] Filippo Santambrogio. Optimal transport for applied mathematicians. 2015.

[17] Carlo A Trugenberger. Combinatorial quantum gravity: geometry from random bits. *Journal of High Energy Physics*, 2017(9):1–8, 2017.

[18] Pim Van Der Hoorn, William J Cunningham, Gábor Lippner, Carlo Trugenberger, and Dmitri Krioukov. Ollivier-ricci curvature convergence in random geometric graphs. *Physical Review Research*, 3(1):013211, 2021.

[19] Christy Kelly, Fabio Biancalana, and Carlo Trugenberger. Convergence of combinatorial gravity. *Physical Review D*, 105(12):124002, 2022.

[20] Carlo A Trugenberger. Combinatorial quantum gravity and emergent 3d quantum behaviour. *Universe*, 9(12):499, 2023.

[21] Richard P Feynman. Simulating physics with computers. In *Feynman and computation*, pages 133–153. CRC Press, 2018.

[22] Paul Benioff. The computer as a physical system: A microscopic quantum mechanical hamiltonian model of computers as represented by turing machines. *Journal of Statistical Physics*, 22:563–591, 1980.

[23] David Deutsch. Quantum theory, the church–turing principle and the universal quantum computer. *Proceedings of the Royal Society of London. A. Mathematical and Physical Sciences*, 400(1818):97–117, 1985.

[24] David Deutsch and Richard Jozsa. Rapid solution of problems by quantum computation. *Proceedings of the Royal Society of London. Series A: Mathematical and Physical Sciences*, 439(1907):553–558, 1992.

[25] Peter W Shor. Polynomial-time algorithms for prime factorization and discrete logarithms on a quantum computer. *SIAM Review*, 41(2):303–332, 1999.

[26] Lov K Grover. A fast quantum mechanical algorithm for database search. In *Proceedings of the twenty-eighth annual ACM Symposium on Theory of Computing*, pages 212–219, 1996.

[27] Bela Bauer, Sergey Bravyi, Mario Motta, and Garnet Kin-Lic Chan. Quantum algorithms for quantum chemistry and quantum materials science. *Chemical reviews*, 120(22):12685–12717, 2020.

[28] Marco Cerezo, Andrew Arrasmith, Ryan Babbush, Simon C Benjamin, Suguru Endo, Keisuke Fujii, Jarrod R McClean, Kosuke Mitarai, Xiao Yuan, Lukasz Cincio, et al. Variational quantum algorithms. *Nature Reviews Physics*, 3(9):625–644, 2021.

[29] Aram W Harrow, Avinatan Hassidim, and Seth Lloyd. Quantum algorithm for linear systems of equations. *Physical Review Letters*, 103(15):150502, 2009.

[30] Andrew M Childs, Robin Kothari, and Rolando D Somma. Quantum algorithm for systems of linear equations with exponentially improved dependence on precision. *SIAM Journal on Computing*, 46(6):1920–1950, 2017.

[31] Leonard Wossnig, Zhikuan Zhao, and Anupam Prakash. Quantum linear system algorithm for dense matrices. *Physical review letters*, 120(5):050502, 2018.

[32] Dominic W Berry, Graeme Ahokas, Richard Cleve, and Barry C Sanders. Efficient quantum algorithms for simulating sparse hamiltonians. *Communications in Mathematical Physics*, 270(2):359–371, 2007.

[33] Dominic W Berry and Andrew M Childs. Blackbox hamiltonian simulation and unitary implementation. *Quantum Information and Computation*, 12:29–62, 2009.

[34] Dominic W Berry. High-order quantum algorithm for solving linear differential equations. *Journal of Physics A: Mathematical and Theoretical*, 47(10):105301, 2014.

[35] Dominic W Berry, Andrew M Childs, and Robin Kothari. Hamiltonian simulation with nearly optimal dependence on all parameters. In *2015 IEEE 56th Annual Symposium on Foundations of Computer Science*, pages 792–809. IEEE, 2015.

[36] Dominic W Berry, Andrew M Childs, Richard Cleve, Robin Kothari, and Rolando D Somma. Simulating hamiltonian dynamics with a truncated taylor series. *Physical Review Letters*, 114(9):090502, 2015.

[37] Seth Lloyd. Universal quantum simulators. *Science*, 273(5278):1073–1078, 1996.

[38] Andrew M Childs, Dmitri Maslov, Yunseong Nam, Neil J Ross, and Yuan Su. Toward the first quantum simulation with quantum speedup. *Proceedings of the National Academy of Sciences*, 115(38):9456–9461, 2018.

[39] Rene Gerritsma, Gerhard Kirchmair, Florian Zähringer, E Solano, R Blatt, and CF Roos. Quantum simulation of the dirac equation. *Nature*, 463(7277):68–71, 2010.

[40] Ryan Babbush, Nathan Wiebe, Jarrod McClean, James McClain, Hartmut Neven, and Garnet Kin-Lic Chan. Low-depth quantum simulation of materials. *Physical Review X*, 8(1):011044, 2018.

[41] Juan Miguel Arrazola, Timjan Kalajdzievski, Christian Weedbrook, and Seth Lloyd. Quantum algorithm for non-homogeneous linear partial differential equations. *Physical Review A*, 100(3):032306, 2019.

[42] Andrew M Childs, Jin-Peng Liu, and Aaron Ostrander. High-precision quantum algorithms for partial differential equations. *Quantum*, 5:574, 2021.

[43] Jin-Peng Liu, Herman Øie Kolden, Hari K Krovi, Nuno F Loureiro, Konstantina Trivisa, and Andrew M Childs. Efficient quantum algorithm for dissipative nonlinear differential equations. *Proceedings of the National Academy of Sciences*, 118(35):e2026805118, 2021.

[44] Hari Krovi. Improved quantum algorithms for linear and nonlinear differential equations. *Quantum*, 7:913, 2023.

[45] Maria Schuld and Francesco Petruccione. *Supervised learning with quantum computers*, volume 17. Springer, 2018.

[46] Maria Schuld, Ville Bergholm, Christian Gogolin, Josh Izaac, and Nathan Killoran. Evaluating analytic gradients on quantum hardware. *Physical Review A*, 99(3):032331, 2019.

[47] Maria Schuld. Machine learning in quantum spaces, 2019.

[48] Maria Schuld and Nathan Killoran. Quantum machine learning in feature hilbert spaces. *Physical Review Letters*, 122(4):040504, 2019.

[49] Maria Schuld, Alex Bocharov, Krysta M Svore, and Nathan Wiebe. Circuit-centric quantum classifiers. *Physical Review A*, 101(3):032308, 2020.

[50] Seth Lloyd, Masoud Mohseni, and Patrick Rebentrost. Quantum algorithms for supervised and unsupervised machine learning. *arXiv preprint arXiv:1307.0411*, 2013.

[51] Vojtěch Havlíček, Antonio D Cárcoles, Kristan Temme, Aram W Harrow, Abhinav Kandala, Jerry M Chow, and Jay M Gambetta. Supervised learning with quantum-enhanced feature spaces. *Nature*, 567(7747):209–212, 2019.

[52] Seth Lloyd, Silvano Garnerone, and Paolo Zanardi. Quantum algorithms for topological and geometric analysis of data. *Nature communications*, 7(1):1–7, 2016.

[53] Dominic W Berry, Yuan Su, Casper Gyurik, Robbie King, Joao Basso, Alexander Del Toro Barba, Abhishek Rajput, Nathan Wiebe, Vedran Dunjko, and Ryan Babbush. Analyzing prospects for quantum advantage in topological data analysis. *PRX Quantum*, 5(1):010319, 2024.

[54] Alexander Schmidhuber and Seth Lloyd. Complexity-theoretic limitations on quantum algorithms for topological data analysis. *PRX Quantum*, 4:040349, Dec 2023.

[55] Nhat A Nghiêm, Xianfeng David Gu, and Tzu-Chieh Wei. Quantum algorithm for estimating betti numbers using a cohomology approach. *arXiv preprint arXiv:2309.10800*, 2023.

[56] Nhat A Nghiêm and Junseo Lee. New aspects of quantum topological data analysis: Betti number estimation, and testing and tracking of homology and cohomology classes. *arXiv preprint arXiv:2506.01432*, 2025.

[57] Ryu Hayakawa. Quantum algorithm for persistent betti numbers and topological data analysis. *Quantum*, 6:873, 2022.

[58] Casper Gyurik, Alexander Schmidhuber, Robbie King, Vedran Dunjko, and Ryu Hayakawa. Quantum computing and persistence in topological data analysis. *arXiv preprint arXiv:2410.21258*, 2024.

[59] Shashanka Ubaru, Ismail Yunus Akhalwaya, Mark S Squillante, Kenneth L Clarkson, and Lior Horesh. Quantum topological data analysis with linear depth and exponential speedup. *arXiv preprint arXiv:2108.02811*, 2021.

[60] Nhat A Nghiêm, Tuan K Do, Tzu-Chieh Wei, and Trung V Phan. Quantum algorithm for estimating intrinsic geometry. *arXiv preprint arXiv:2508.06355*, 2025.

[61] Tristan Luca Saidi, Abigail Hickok, and Andrew J Blumberg. Recovering manifold structure using ollivier-ricci curvature. *arXiv preprint arXiv:2410.01149*, 2024.

[62] Emil Saucan, RP Sreejith, RP Vivek-Ananth, Jürgen Jost, and Areejit Samal. Discrete ricci curvatures for directed networks. *Chaos, Solitons & Fractals*, 118:347–360, 2019.

[63] Nazanin Azarhooshang, Prithviraj Sengupta, and Bhaskar DasGupta. A review of and some results for ollivier-ricci network curvature. *Mathematics*, 8(9), 2020.

[64] Vašek Chvátal. *Linear programming*. Macmillan, 1983.

[65] George B Dantzig. Linear programming. *Operations research*, 50(1):42–47, 2002.

[66] James Orlin. A faster strongly polynomial minimum cost flow algorithm. In *Proceedings of the Twentieth Annual ACM Symposium on Theory of Computing*, pages 377–387, 1988.

[67] Li Chen, Rasmus Kyng, Yang Liu, Richard Peng, Maximilian Probst Gutenberg, and Sushant Sachdeva. Maximum flow and minimum-cost flow in almost-linear time. *Journal of the ACM*, 72(3):1–103, 2025.

[68] Albert W. Marshall, Ingram Olkin, and Barry C. Arnold. Inequalities: theory of majorization and its applications. 1979.

[69] Garrett Birkhoff. Three observations on linear algebra. *Univ. Nac. Tacuman, Rev. Ser. A*, 5:147–151, 1946.

[70] Harold W. Kuhn. The Hungarian method for the assignment problem. *Naval research logistics quarterly*, 2(1–2):83–97, 1955.

[71] Abigail Hickok and Andrew J Blumberg. An intrinsic approach to scalar-curvature estimation for point clouds. *arXiv preprint arXiv:2308.02615*, 2023.

[72] András Gilyén, Yuan Su, Guang Hao Low, and Nathan Wiebe. Quantum singular value transformation and beyond: exponential improvements for quantum matrix arithmetics. In *Proceedings of the 51st Annual ACM SIGACT Symposium on Theory of Computing*, pages 193–204, 2019.

[73] Guang Hao Low and Isaac L Chuang. Optimal hamiltonian simulation by quantum signal processing. *Physical Review Letters*, 118(1):010501, 2017.

[74] Guang Hao Low and Isaac L Chuang. Hamiltonian simulation by qubitization. *Quantum*, 3:163, 2019.

[75] Shantanav Chakraborty, András Gilyén, and Stacey Jeffery. The power of block-encoded matrix powers: improved regression techniques via faster hamiltonian simulation. *arXiv preprint arXiv:1804.01973*, 2018.

[76] Nhat A Nghiêm and Tzu-Chieh Wei. Improved quantum algorithms for eigenvalues finding and gradient descent. *arXiv preprint arXiv:2312.14786*, 2023.

[77] Nhat A Nghiêm, Hiroki Sukeno, Shuyu Zhang, and Tzu-Chieh Wei. Improved quantum power method and numerical integration using a quantum singular-value transformation. *Physical Review A*, 111(1):012434, 2025.

[78] Sam McArdle, András Gilyén, and Mario Berta. Quantum state preparation without coherent arithmetic. *arXiv preprint arXiv:2210.14892*, 2022.

[79] Xiao-Ming Zhang, Tongyang Li, and Xiao Yuan. Quantum state preparation with optimal circuit depth: Implementations and applications. *Physical Review Letters*, 129(23):230504, 2022.

[80] Vivek V Shende, Stephen S Bullock, and Igor L Markov. Synthesis of quantum logic circuits. In *Proceedings of the 2005 Asia and South Pacific Design Automation Conference*, pages 272–275, 2005.

[81] Adriano Barenco, Charles H Bennett, Richard Cleve, David P DiVincenzo, Norman Margolus, Peter Shor, Tycho Sleator, John A Smolin, and Harald Weinfurter. Elementary gates for quantum computation. *Physical review A*, 52(5):3457, 1995.

[82] Gabriel Marin-Sánchez, Javier Gonzalez-Conde, and Mikel Sanz. Quantum algorithms for approximate function loading. *Physical Review Research*, 5(3):033114, 2023.

[83] Kouhei Nakaji, Shumpei Uno, Yohichi Suzuki, Rudy Raymond, Tamiya Onodera, Tomoki Tanaka, Hiroyuki Tezuka, Naoki Mitsuda, and Naoki Yamamoto. Approximate amplitude encoding in shallow parameterized quantum circuits and its application to financial market indicators. *Physical Review Research*, 4(2):023136, 2022.

[84] Christa Zoufal, Aurélien Lucchi, and Stefan Woerner. Quantum generative adversarial networks for learning and loading random distributions. *npj Quantum Information*, 5(1):103, 2019.

[85] Junseo Lee and Nhat A Nghiêm. New aspects of quantum topological data analysis: Betti number estimation, and testing and tracking of homology and cohomology classes. *arXiv preprint arXiv:2506.01432*, 2025.

[86] Daan Camps and Roel Van Beeumen. Approximate quantum circuit synthesis using block encodings. *Physical Review A*, 102(5):052411, 2020.

Appendix A: Calculating ORC

Here we show the concrete steps required to estimate the ORC associated with edge (x, y) of the graph in Fig. 1. The geodesic distances between pairs of relevant points for this calculation are:

$$\begin{aligned} d_G(x_1, y_1) &= 1, \quad d_G(x_1, y_2) = 3, \quad d_G(x_1, y_3) = 3, \quad d_G(x_1, y_4) = 2, \\ d_G(x_2, y_1) &= 2, \quad d_G(x_2, y_2) = 3, \quad d_G(x_2, y_3) = 3, \quad d_G(x_2, y_4) = 3, \\ d_G(x_3, y_1) &= 3, \quad d_G(x_3, y_2) = 2, \quad d_G(x_3, y_3) = 2, \quad d_G(x_3, y_4) = 3. \end{aligned} \quad (\text{A.1})$$

We need to find the non-negative $3 \times 4 = 12$ values $\{\gamma_{ij}\}_{i=1, j=1}^{3,4}$ that minimize the following linear combination:

$$\begin{aligned} \mathcal{W}(\{\gamma_{ij}\}) &= d_G(x_1, y_1)\gamma_{11} + d_G(x_1, y_2)\gamma_{12} + d_G(x_1, y_3)\gamma_{13} + d_G(x_1, y_4)\gamma_{14} + \\ &\quad d_G(x_2, y_1)\gamma_{21} + d_G(x_2, y_2)\gamma_{22} + d_G(x_2, y_3)\gamma_{23} + d_G(x_2, y_4)\gamma_{24} + \\ &\quad d_G(x_3, y_1)\gamma_{31} + d_G(x_3, y_2)\gamma_{32} + d_G(x_3, y_3)\gamma_{33} + d_G(x_3, y_4)\gamma_{34} \\ &= \gamma_{11} + 3\gamma_{12} + 3\gamma_{13} + 2\gamma_{14} + 2\gamma_{21} + 3\gamma_{22} + \\ &\quad 3\gamma_{23} + 3\gamma_{24} + 3\gamma_{31} + 2\gamma_{32} + 2\gamma_{33} + 3\gamma_{34}, \end{aligned} \quad (\text{A.2})$$

subjected to the constraints:

$$\begin{aligned} &\gamma_{11} + \gamma_{12} + \gamma_{13} + \gamma_{14} \\ &= \gamma_{21} + \gamma_{22} + \gamma_{23} + \gamma_{24} \\ &= \gamma_{31} + \gamma_{32} + \gamma_{33} + \gamma_{34} = 1/3 \end{aligned} \quad (\text{A.3})$$

and

$$\begin{aligned} &\gamma_{11} + \gamma_{21} + \gamma_{31} \\ &= \gamma_{12} + \gamma_{22} + \gamma_{32} \\ &= \gamma_{13} + \gamma_{23} + \gamma_{33} \\ &= \gamma_{14} + \gamma_{24} + \gamma_{34} = 1/4. \end{aligned} \quad (\text{A.4})$$

The minimum value of \mathcal{W} can be found to be $25/12$, located at

$$\gamma_{11} = 1/4, \quad \gamma_{14} = 1/12, \quad \gamma_{23} = 1/6, \quad \gamma_{24} = 1/6, \quad \gamma_{32} = 1/4, \quad \gamma_{33} = 1/12,$$

and other γ -values are 0. From this result, we can use Eq. (II.3) to estimate the Earth Mover distance

$$W_1(x, y) = \min_{\{\gamma_{ij}\}} \mathcal{W}(\{\gamma_{ij}\}) = 25/12.$$

The geodesic distance between point x and point y is of unit-length, i.e. $d_G(x, y) = 1$, therefore we can obtain the estimated ORC value from Eq. (II.2):

$$\gamma(x, y) = 1 - \frac{W_1(x, y)}{d_G(x, y)} = 1 - \frac{25/12}{1} = -\frac{13}{12}. \quad (\text{A.5})$$

Appendix B: Block-encoding and quantum singular value transformation

We briefly summarize the essential quantum tools used in our algorithm. For conciseness, we highlight only the main results and omit technical details, which are thoroughly covered in [72]. An identical summary is also presented in [85].

Definition B.1 (Block-encoding unitary, see e.g. [72–74]). *Let A be a Hermitian matrix of size $N \times N$ with operator norm $\|A\| < 1$. A unitary matrix U is said to be an exact block encoding of A if*

$$U = \begin{pmatrix} A & * \\ * & * \end{pmatrix}, \quad (\text{B.1})$$

where the top-left block of U corresponds to A . Equivalently, one can write

$$U = |\mathbf{0}\rangle\langle\mathbf{0}| \otimes A + (\dots), \quad (\text{B.2})$$

where $|\mathbf{0}\rangle$ denotes an ancillary state used for block encoding, and (\dots) represents the remaining components orthogonal to $|\mathbf{0}\rangle\langle\mathbf{0}| \otimes A$. If instead U satisfies

$$U = |\mathbf{0}\rangle\langle\mathbf{0}| \otimes \tilde{A} + (\dots), \quad (\text{B.3})$$

for some \tilde{A} such that $\|\tilde{A} - A\| \leq \epsilon$, then U is called an ϵ -approximate block encoding of A . Furthermore, the action of U on a state $|\mathbf{0}\rangle|\phi\rangle$ is given by

$$U|\mathbf{0}\rangle|\phi\rangle = |\mathbf{0}\rangle A|\phi\rangle + |\text{garbage}\rangle, \quad (\text{B.4})$$

where $|\text{garbage}\rangle$ is a state orthogonal to $|\mathbf{0}\rangle A|\phi\rangle$. The circuit complexity (e.g., depth) of U is referred to as the complexity of block encoding A .

Based on B.1, several properties, though immediate, are of particular importance and are listed below.

Remark B.1 (Properties of block-encoding unitary). *The block-encoding framework has the following immediate consequences:*

- (i) Any unitary U is trivially an exact block encoding of itself.
- (ii) If U is a block encoding of A , then so is $\mathbb{I}_m \otimes U$ for any $m \geq 1$.
- (iii) The identity matrix \mathbb{I}_m can be trivially block encoded, for example, by $\sigma_z \otimes \mathbb{I}_m$.

Given a set of block-encoded operators, various arithmetic operations can be done with them. Here, we simply introduce some key operations that are especially relevant to our algorithm, focusing on how they are implemented and their time complexity, without going into proofs. For more detailed explanations, see [72, 86].

Lemma B.1 (Informal, product of block-encoded operators, see e.g. [72]). *Given unitary block encodings of two matrices A_1 and A_2 , with respective implementation complexities T_1 and T_2 , there exists an efficient procedure for constructing a unitary block encoding of the product $A_1 A_2$ with complexity $T_1 + T_2$.*

Lemma B.2 (Informal, tensor product of block-encoded operators, see e.g. [86, Theorem 1]). *Given unitary block-encodings $\{U_i\}_{i=1}^m$ of multiple operators $\{M_i\}_{i=1}^m$ (assumed to be exact), there exists a procedure that constructs a unitary block-encoding of $\bigotimes_{i=1}^m M_i$ using a single application of each U_i and $\mathcal{O}(1)$ SWAP gates.*

Lemma B.3 (Informal, linear combination of block-encoded operators, see e.g. [72, Theorem 52]). *Given the unitary block encoding of multiple operators $\{A_i\}_{i=1}^m$. Then, there is a procedure that produces a unitary block encoding operator of $\sum_{i=1}^m \pm(A_i/m)$ in time complexity $\mathcal{O}(m)$, e.g., using the block encoding of each operator A_i a single time.*

Lemma B.4 (Informal, Scaling multiplication of block-encoded operators). *Given a block encoding of some matrix A , as in B.1, the block encoding of A/p where $p > 1$ can be prepared with an extra $\mathcal{O}(1)$ cost.*

Lemma B.5 (Matrix inversion, see e.g., [30, 72]). *Given a block encoding of some matrix A with operator norm $\|A\| \leq 1$ and block-encoding complexity T_A , then there is a quantum circuit producing an ϵ -approximated block encoding of A^{-1}/κ where κ is the conditional number of A . The complexity of this quantum circuit is $\mathcal{O}(\kappa T_A \log(1/\epsilon))$.*